55th Annual Midwest Student Biomedical Research Forum

Saturday, March 2, 2024

ROOM 3040

1:45 p.m. **O-06** DECODING GENOME-WIDE TF-CHROMATIN INTERACTION DYNAMICS
Presenter: Soumi Basu, UNMC

2:00 p.m. **O-13** NORTRIPTYLINE TRIGGERS APOPTOSIS IN GROUP 3 MEDULLOBLASTOMA BY INDUCING MITOCHONDRIAL DYSFUNCTION
Presenter: David Doss, Creighton University

2:15 p.m. **O-15** BACTERIAL METALLOPHORES AND ZINC DEFICENCY INCREASE THE SEVERITY OF INFLAMMATORY BOWEL DISEASE
Presenter: Christi Ellis, UNMC

2:30 p.m. **O-17** HOMOLOGOUS RECOMBINATION-RELEVANT PHOSPHOMIMETICS OF REPLICATION PROTEIN A
Presenter: Valerie Fousek-Schuller, UNMC

2:45 p.m. **O-28** CRUSH: AN ALGORITHM TO IDENTIFY FINE-SCALE COMPARTMENTS IN Hi-C MAPS
Presenter: Achyuth Kalluchi, UNMC

3:00 p.m. **O-30** CDC25A-DERIVED PHOSPHOPEPTIDES BIND 14-3-3ε WITH HIGH AFFINITY
Presenter: Seraphine Kamayirese, Creighton University

3:15 p.m. **O-40** RE-CLASSIFICATION OF *PMS2* KOZAK SEQUENCE VARIANTS USING A FAST AND RELIABLE *IN VITRO* ASSAY
Presenter: Evanjalina Matoy, Creighton University

3:30 p.m. **O-59** JUKEBOX: QUANTIFYING NOISE IN CHROMATIN COFORMATION CAPTURE MATRICES
Presenter: Timothy Reznicek, UNMC

3:45 p.m. **O-62** ESTABLISHING MOLECULAR REQUIREMENTS FOR ERYTHROID PROGENITOR ACTIVATION DURING ANEMIA RECOVERY
Presenter: Pooja Roy, UNMC

4:00 p.m. Break

DECODING GENOME-WIDE TF-CHROMATIN INTERACTION DYNAMICS

Soumi Basu, Jim Persinger, Sandipan Brahma
University of Nebraska Medical Center, Omaha

Background: The SWI/SNF family ATP-dependent chromatin remodeling complex BAF (BRG1/BRM-Associated Factor) is a key regulator of chromatin structure and transcription in mammals, and mutations in BAF is implicated in ~25% of cancers. BAF expels genomic nucleosomes to form nucleosome depleted regions (NDR) and facilitates transcription factor (TF) binding to enable gene transcription, thereby regulating a myriad of cellular functions. More than hundred TFs are expressed in every cell type, and their individual or combined action drives locus- and cell-type-specific gene expression. Structural motifs within TFs such as leucine zipper, zinc finger, homeodomain, and helix-turn-helix loops capacitate their interaction with DNA. Therefore, on chromatin, TF function is modulated by the accessibility and presentation of their cognate DNA sequence motifs. We use a combination of high-resolution genome-wide mapping and chemical genetics approach to comprehensively characterize how chromatin remodeling by BAF regulates distinct TF families and their interaction with chromatin.

Significance: Our project is a comprehensive examination of how BAF regulates TF-chromatin transactions genome-wide in murine embryonic stem cell (mESC) pluripotency and during early embryonic development. TF-chromatin interactions drive cell-type-specific gene expression in development and is often deregulated in cancer. Our study broadly reveals mechanisms regulating locus- and cell-type-specific chromatin structure, a critical aspect of epigenetic gene regulation.

Question: Although both BAF and TF function are important for gene regulation, the role of BAF nucleosome remodeling in regulating distinct TF families and modes of chromatin binding is unclear.

Experimental Design and Results: We use the high-resolution genome wide mapping techniques CUT&Tag and CUT&RUN.ChIP to determine the occupancy of BAF and TFs genome wide in mESC, as well as the substructure and composition of genomic nucleosomes associated with these factors. We find that BAF partially unwraps nucleosomes to dynamically expose pluripotency TF binding sites. We show that mild overexpression of the pluripotency TFs NANOG and KLF4 drive the eviction of these partially unwrapped nucleosome remodeling intermediates, suggesting that pluripotency TFs capture transiently exposed DNA sequences for chromatin binding and nucleosome eviction. We will further determine whether and how inhibition of BAF remodeling regulate distinct TFs families using a specific ATPase inhibitor BRM014, and a PROTAC protein degrader ASBI1, both targeting the BRG1 subunit of the BAF complex. We will use MNase-seq along with a computational approach for differential fragment-length analysis over TF motifs to determine distinct modes of TF chromatin interactions. We will further validate MNase-seq results by CUT&RUN.ChIP targeting specific TFs.

Conclusion: We show that the homeobox TF NAGOG and zinc finger TF KLF4 capture transiently exposed DNA sequences due to BAF remodeling nucleosomes to drive nucleosome eviction. Our ongoing work will reveal the mechanisms by which other TF families interact with chromatin.

NORTRIPTYLINE TRIGGERS APOPTOSIS IN GROUP 3 MEDULLOBLASTOMA BY INDUCING MITOCHONDRIAL DYSFUNCTION

David Doss[1], Ranjana K Kanchan[2], Naveenkumar Perumal[2], Surinder Batra[2], Sidharth Mahapatra[2,3]
[1] *Creighton University School of Medicine, Department of Biomedical Sciences, Omaha, NE*
[2] *University of Nebraska Medical Center, Department of Biochemistry and Molecular Biology, Omaha, NE*
[3] *Children's Hospital & Medical Center, Department of Pediatrics, Omaha, NE*

Background: Medulloblastoma (MB) is the most common malignant brain tumor of childhood and is divided into four primary subgroups based on unique molecular features. Group 3 (G3) MB tumors comprise 25% of all MB by incidence and are the most aggressive. Despite ongoing efforts to improve outcomes, patients with G3MB tumors have 5-year overall survival rates of <50%, compared to the other subgroups with survival rates ranging from 70-95%. The current standard of care for G3MB consists of maximal safe surgical resection with subsequent craniospinal irradiation and systemic chemotherapy consisting of cisplatin, cyclophosphamide, vincristine, and lomustine.

Significance: Given the application of similar treatments across molecularly-divergent tumors, subgroup-specific prognoses vary widely. For high-risk tumors like G3MB, toxicities associated with the use of high-dose systemic chemotherapy and craniospinal irradiation in childhood either contribute to late morbidity and mortality or limit therapy, leading to recurrence. This conundrum underlies the need to minimize the use of nonspecific cytotoxic therapies in a vulnerable population, specifically for G3 MB, the subgroup with the worst prognosis. Recent efforts to target MB with subgroup-specific therapies have shown mixed results; precise administration of craniospinal irradiation and repurposed hedgehog pathway inhibitors have improved outcomes in the WNT and SHH subgroups of MB, respectively, yet only incremental progress has been made for G3MB, mostly focused on targeting the aberrant methylation profiles seen in this subgroup via histone deacetylase inhibitors. As such, we are pursuing an alternative *a priori* approach to drug discovery, starting with our library of patient-derived subgroup-specific RNA-sequencing data.

Hypothesis: We hypothesize that nortriptyline (NT) is a viable, repositionable candidate for the treatment of G3MB which acts to induce apoptosis through a mitochondrial-dependant mechanism.

Experimental Design: In this study, we compared RNA sequencing data for G3MB against a drug transcriptomic signature database to identify FDA-approved drugs capable of reversing the G3MB expression profile in an effort to identify novel drugs with treatment efficacy. We performed differential expression analysis on two RNA sequencing datasets: a local cohort of MB samples from pediatric patients (GSE148389; normal cerebellum n=14, MB n=26, G3 n=7) and an external validation dataset similarly consisting of MB samples (GSE164677; normal cerebellum n=4, MB n=63, G3 n=14). We then assessed these data against the LINCS perturbagen database, which consists of gene expression signatures of over seventy human cell lines before and after treatment with over 42,000 perturbagens. This pipeline allowed us to identify hundreds of mutually discordant compounds across the two RNA sequencing datasets, each with the potential to reverse the gene expression signature seen in G3MB to a signature more similar to the normal cerebellum. We then applied a modified version of Lipinski's Rules of 5 to filter candidate compounds for oral bioavailability and the potential to cross the blood-brain barrier based on molecular characteristics. We also filtered candidates for FDA-approval status using the DrugBank database. Upon determining the top candidates *in silico*, we performed functional assays to quantify the drugs' effects on cytotoxicity, clonogenicity, wound healing, migration and invasion, and apoptosis *in vitro* in the G3 MB cell lines HDMB03 and D425. Following confirmation of functional efficacy, we proceeded to characterize the mechanism of action of our top candidate compound through RNA sequencing.

Results: One hundred and six candidate compounds passed preliminary filtering thresholds and qualified for further testing. We screened the list of qualifying compounds and identified thirteen core compounds with favorable safety profiles in a pediatric population. The cytotoxic IC_{50} of each compound was determined through an MTT assay. Of these compounds, three classes of drugs consistently ranked among the top candidates: selective serotonin reuptake inhibitors (SSRIs), statins, and tricyclic antidepressants (TCAs). Results from MTT assays demonstrated 48h IC_{50} values in the low micromolar range for our top compounds of interest, including NT (7.0μM). NT abrogated colony formation during *in vitro* clonogenic assays at the IC_{50} value. Additionally, NT demonstrated a dose- and time-dependent reduction in cell migration through a 2D wound healing ("scratch") assay and a 3D tumor spheroid assay. Flow cytometry of cells stained with Annexin V and propidium iodide demonstrated a dose- and time-dependent increase in apoptotic cells relative to control when treated with NT. To support these data, induction of apoptosis was confirmed by probing for key markers of intrinsic apoptosis on Western blot; namely, cleaved caspase 3, cleaved PARP, and BCL-2. RNA-sequencing of HDMB03 cells treated with NT revealed suppression of pathways related to mitochondrial metabolism alongside upregulation of lipid metabolism.

Conclusions: Taken together, we have successfully used our pipeline to identify compounds that are actively cytotoxic against G3MB cells *in vitro*. NT has shown the most consistent anti-neoplastic trend in all *in vitro* assays. We plan to carry out further *in vitro* studies to investigate the potential for synergy with existing MB chemotherapy agents and characterize the mitochondrial mechanism of NT. We will also test our drugs *in vivo* to assess their impact on tumor burden and survival. Overall, this pipeline provides a useful model for identifying repurposable FDA-approved drugs, which can be quickly made available to patients and clinicians, particularly given the widespread public availability of gene expression data and the current widening gap in survivorship for G3 MB patients.

BACTERIAL METALLOPHORES AND ZINC DEFICENCY INCREASE THE SEVERITY OF INFLAMMATORY BOWEL DISEASE

C.M. Ellis[1], D.N. Villageliu[1], K.C. Cunningham[1], D.L. Knoell[2], and D.R., Samuelson[1, 3]

Departments of [1]Internal Medicine-Pulmonary Division, and [2]Pharmacy Practice and Science, University of Nebraska Medical Center, Omaha, NE, USA; [3]Nebraska Food for Health Center, University of Nebraska-Lincoln, Lincoln, NE, USA.

Introduction: Zinc (Zn) deficiency has emerged as a growing public health problem. In fact, an estimated 17% of the global population is at risk of inadequate Zn intake. Animal studies have demonstrated that even marginal Zn deprivation leads to significantly impaired physiological functions. While Zn is required for optimal cellular functions throughout the body, the gastrointestinal tract is particularly vulnerable to Zn depletion, as maintenance of intestinal homeostasis, as well as the resident microbiota require Zn. Zn deficiency mediated loss of intestinal homeostasis and microbial dysbiosis have recently been proposed as major mechanistic pathways for the development and severity of inflammatory bowel disease (IBD). Genetics, microbial composition, and dietary Zn levels are associated with accelerated IBD severity on an individual basis; however, the interaction and crosstalk among these factors in IBD pathogenesis remains to be elucidated. We propose that microbiota-associated metallophores are the key link between genetics, intestinal microbiota, and Zn in the severity of IBD. Specifically, we hypothesize that IBD disease status is associated with a unique subset of microbial metallophores; we further hypothesize that IBD-associated metallophores exacerbate disease severity.

Method: We utilized both in vivo and in vitro models to investigate the relationship between zinc deficiency, microbial metallophores, and IBD severity. We utilized the gold standard IBD in vivo model (*Dextran sodium sulfate colitis*), coupled with our standard dietary manipulation of Zn. Specifically, mice were placed on either a zinc deficient (1ppm) or zinc sufficient diet for 3 weeks prior to the initiation of DSS colitis. Mice were treated with 2.5% DSS in their drinking water for 5 days and sacrificed. We also utilized our standard DSS model coupled with Zn supplementation with Zinpro. Mice were gavaged daily with 200 μg/dose of Zinpro starting at day 2 of DSS treatment. In addition, to Zn supplementation select groups of mice were gavaged with Adherent-invasive *E. coli* ($1x10^8$ CFU) three times, on days four and five of DSS treatment, and one day post DSS to mimic a pathobiont bloom following an IBD flare. Finally, we performed in vitro Zinpro dose-response growth curves using both AIEC and *Lactobacillus rhamnosus*. We assessed the effects of both Zn supplementation and deficiency in our animal models using three primary outcomes: 1) increases/decreases in Disease Activity index, 2) improvements in organ (colon, liver, spleen) gross pathology, and 3) changes in the microbiota expression of metallophores.

Results: We found that on a zinc deficient diet, colitis severity and mortality were significantly increased. This was associated with a marked increase in the expression of GI-microbiota metalllophores (enterobactin, yersinobactin, and salmochelin) in DSS treated mice. Zn deficient diets increase the expression of microbiota-metallophores in both DSS and water treated mice. AIEC also exacerbates DSS-colitis, which may be due to E. coli's production of metallophores, and the increased intestinal burden of AIEC colonization. Most strikingly, we found that Zinpro supplementation impairs AIEC growth but not lactobacillus growth, and drastically improves DSS-mediated colitis, improves gross pathology, and decreases luminal and intracolonic AIEC burden.

Conclusion: Together this data suggests that zinc deficiency exacerbates IBD due in part to the increased metallophore burden in the GI. Zinc supplementation during DSS-colitis improves the disease severity and pathobiont (AIEC) burden.

HOMOLOGOUS RECOMBINATION-RELEVANT PHOSPHOMIMETICS OF REPLICATION PROTEIN A

Valerie Fousek-Schuller[1], Lucas Struble[2], Mona Al-Mugotir[2], Carol Kolar[2], & Gloria E. O. Borgstahl[2]

[1]Immunology, Pathology, and Infectious Diseases, [2]Eppley Institute for Research in Cancer & Allied Diseases, UNMC, Omaha, NE

Background

Homologous recombination (HR) repairs DNA double-strand breaks (DSBs), which can be deficient in cancer cells. Heterotrimeric replication protein A (RPA), the main single-stranded DNA-binding protein in humans, is essential for cellular DNA metabolism and DNA damage signalling. It has been known that several N-terminal residues of RPA32 are phosphorylated in the DNA damage response (DDR), and more recently, that RPA70 and RPA14 are also phosphorylated. RPA is indispensable for HR-based DSB repair, and phosphorylation regulates activity. Both RPA and RAD52 are critical for single strand annealing. RAD52 is synthetically lethal with BRCA2, BRCA1, and PALB2.

Significance and Hypothesis

Our studies show that the hyperphosphorylation of RPA regulates structure and function of the RPA:RAD52 complex. RPA phosphorylation controls which protein is holding the ssDNA. Due to its importance, complexity, and limited understanding, we have continued to study the hyperphosphorylated forms of RPA using phosphomimetics. We hypothesize that phosphorylation of RPA is a regulatory mechanism with a structure-function relationship.

Experimental Design and Results

Our previous studies showed HR-relevant phosphorylation sites on RPA heterotrimers in G2 and S phase. RPA is always a phosphoprotein and in control cells the heterotrimer had three major isoforms having 1, 2, or 4 phosphates, respectively. In DNA damaged cells, the number of isoforms increased to nine and included up to fourteen phosphorylation sites. In the current study, eleven candidate DDR phosphorylation sites on RPA70 and RPA32 were determined and systematically mutated to Glu. The expression and purification of >15 combinations of RPA heterotrimers containing phosphomimetics were explored. Effects on activity of these RPA phosphomimetic heterotrimers will be evaluated with surface plasmon resonance (SPR) to determine binding affinity of RPA to ssDNA and RAD52. RPA secondary structures of WT and mutants will be explored with circular dichroism (CD). These studies will focus on the regulatory role of phosphorylation on the macromolecular complexes that process and repair DSBs.

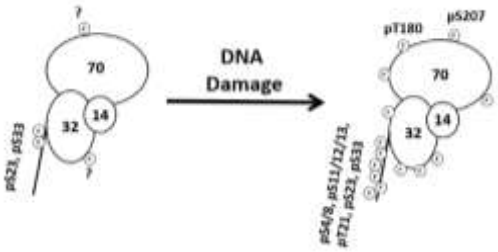

Conclusion

RPA phosphorylation plays a critical role in DNA metabolism, specifically in DNA repair. Understanding how phosphorylation of RPA regulates these various pathways in DNA repair, we can create phosphomimetics for the RPA:RAD52 interaction that could inhibit this interaction involving the alternate HR pathways in BRCA2 complex deficient cells, while NOT affecting normal cells.

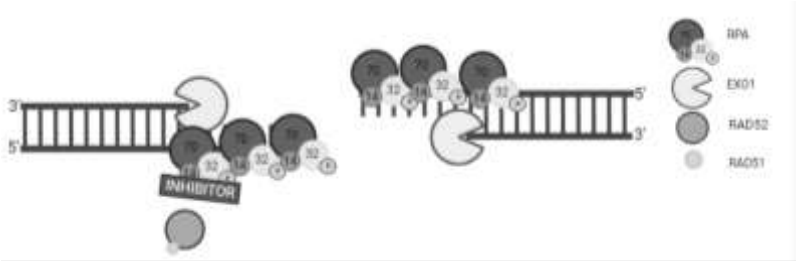

CRUSH: AN ALGORITHM TO IDENTIFY FINE-SCALE COMPARTMENTS IN Hi-C MAPS

Achyuth Kalluchi[1], Jordan Rowley[1]
[1]Department of Genetics, Cell Biology and Anatomy, University of Nebraska Medical Center, Omaha, NE, USA.

Advancements in next-generation sequencing and chromatin conformation assays, particularly Hi-C, have helped uncover features of chromatin organization at unprecedented resolution. A prominent feature of chromatin contact maps is the genome segregation of active from inactive compartments into A and B compartments. Identification of these compartmental interaction states is one of the most common and critical parts of Hi-C data analysis. Recent studies have shown that A/B compartments are much smaller than previously thought, such that some compartments consist of single promoters or enhancers and are only a few kilobases (kb) in size. Currently, A/B interactions are commonly identified in Hi-C maps using an Eigenvector-based algorithm which requires high read depth at long distances, thus making it financially prohibitive for wide-spread fine-scale analysis. Indeed, current tools require extreme sequencing depth, i.e., >7 billion contacts, to identify compartments at 500bp resolution. To enable compartment identification, quantification, and differential analysis at high resolution in maps with realistically achievable sequencing depths (~100 million contacts), we developed CRUSH (Compartmental Refinement for Ultraprecise Stratification in Hi-C). This tool represents a robust and versatile compartment caller that reveals new aspects of chromatin organization, compartmental organization specific to different disease states, and novel relationships between transcription and localizing to the A compartment.

CDC25A-DERIVED PHOSPHOPEPTIDES BIND 14-3-3ε WITH HIGH AFFINITY

Seraphine Kamayirese, Sibaprasad Maity, Laura A. Hansen and Sándor Lovas

Department of Biomedical Sciences, School of Medicine, Creighton University, Omaha, NE

In cutaneous squamous cell carcinoma (cSCC), 14-3-3ε protein is overexpressed and mislocalized from the nucleus to the cytoplasm. Like 14-3-3ε, the cell cycle regulator CDC25A is over expressed in cSCC, and it binds to the cytosolic 14-3-3ε protein with phospho-Ser178 or phospho-Thr507 residues. The 14-3-3ε - CDC25A interaction is associated with resistance to apoptosis in cSCC, thus, inhibition of the 14-3-3ε - CDC25A interaction is a promising target for the development of therapeutics for cSCC. Our aim is to develop peptides that inhibit the binding of CDC25A to 14-3-3ε to promote apoptosis of cSCC cells. The previous work by this group developed novel peptides; Ac-CDC25A(502-515)-NH_2 (pT), and Ac-CDC25A(173-186)-NH_2 (pS) corresponding to two binding regions of CDC25A to 14-3-3 proteins. Both pT and pS bind 14-3-3ε, and induce cell death of cSCC cells with IC_{50} of 22.1 μM and 29 μM, respectively. In the current work, we modified the pT and pS peptides to improve their binding affinities for 14-3-3ε, thus, promoting apoptosis in cSCC.

Using molecular modeling and molecular dynamics (MD) simulations, both the pT and pS peptides were sequentially truncated to obtain their 9 amino acid residue analogs, pT(502–510) and pS(174-182), respectively. Based on preferential binding motif of 14-3-3ε client proteins and Ala-scanning, studies, the peptides were modified at different positions, one residue at a time. Free energies of binding (ΔG_b) of the peptide analogs to 14-3-3ε were determined using steered molecular dynamics simulations (SMD). Differential scanning fluorimetry (DSF) was used to determine effect of the peptides on melting temperature (T_m) of 14-3-3ε, and binding affinity (K_D) of the peptides for 14-3-3ε was quantified using surface plasmon resonance (SPR). To elucidate whether the modifications affect secondary structure of the peptides, electronic circular dichroism (ECD) spectropolarimetry was used to determine secondary structures of the peptides in water and in different concentrations of 2,2,2- trifluoroethanol (TFE). Proteolytic stability of pT(502-510) was determined by incubating it with pronase, and digestion products were identified by LC-MS.

SMD results showed that all pT and pS peptide analogs bound 14-3-3ε with negative ΔG_b. DSF results showed that pT analogs caused change in melting temperature (ΔT_m) of 2.43–5.19 °C, while pS peptide analogs led to ΔT_m of 14-3-3ε of 0.3-1.8 °C, except the parent pS peptide that did not show any effect on melting temperature of the protein. SPR data indicated that pT analogs bound 14-3-3ε with K_D in the range of 22.0–144.3 nM, and the pS analogs bound the protein with K_D of 291–6563 nM. Analysis of the ECD spectra of pT(502-510) analogs showed that, in water, secondary structure of the peptides is predominantly random coil with some turn, strand and helical conformations. At high percentages of TFE, the peptides became more structured. Analysis of proteolytic digestion showed that the peptide was cleaved at Lys^{504}-Ser^{505} and Ser^{505}-Arg^{506} bonds.

Our results show that shortening the pT peptide improved its binding affinity (K_D) for 14-3-3ε, and aromatic substitutions at the *C*-terminus of pT(502-510) led to further improvement in the affinity of the peptide. Shortening the pS peptide reduced its affinity for 14-3-3ε, however, the affinity was restored by introducing Lys in position 176. Unnatural amino acids will be introduced at scissile peptide bonds in pT(502-510) to improve proteolytic stability of the analogs. The ability of high affinity, proteolytically stable peptide analogs, to induce apoptosis will be investigated in cSCC cells.

TITLE: RE-CLASSIFICATION OF *PMS2* KOZAK SEQUENCE VARIANTS USING A FAST AND RELIABLE *IN VITRO* ASSAY.

Evanjalina Matoy [1], Jocelyn N. Plowman [1], Michael Belshan [2], Holly A. F. Stessman [1]

[1] Department of Pharmacology & Neuroscience, [2] Department of Medical Microbiology and Immunology, School of Medicine, Creighton University, Omaha, Nebraska, U.S.A.

Background: Lynch Syndrome (LS) is the most common hereditary cancer syndrome affecting 1 in 279 people. Heterozygous loss-of-function variants in PMS2 are linked to LS. While these variants are not directly cancer initiating, PMS2 functions in the DNA mismatch repair pathway such that reduced function results in the accumulation of somatic variants and increased cancer risk over time. We recently identified a suspected hereditary cancer family carrying a 5' UTR variant in PMS2 (ENST00000265849.7: c.-7T>C; MAF: 0.00032 across all races) that had conflicting interpretations of pathogenicity in ClinVar. This variant lies within the Kozak sequence of PMS2, the well-described protein translation initiation motif in eukaryotes. This sequence is highly conserved among higher eukaryotes and is defined as the 10-13 basepairs upstream of the translation start codon through the first 4 bases of the translated sequence (5'-GTTGCATCCATGG-3'; human PMS2 NM_000535.7). Variants in the Kozak sequence have been shown to reduce the translation of genes such as those necessary for heart development resulting in congenital heart disease.

Significance of Problem: All Kozak sequence untranslated variants in PMS2 in ClinVar are currently classified as variants of undetermined significance (VOUSs) due to a paucity of research on this non-coding region.

Hypothesis: We hypothesized that variants that significantly disrupt the Kozak sequence motif of PMS2 would decrease PMS2 protein expression, contributing to increased cancer risk over time.

Experimental Design: Using the psiCHECK™-2 dual luciferase vector (Promega) and site-directed mutagenesis, we modified the endogenous renilla luciferase Kozak sequence (but not the firefly luciferase sequence) to the human PMS2 sequence. A second round of mutagenesis was similarly used to generate ClinVar PMS2 Kozak sequence variants. Plasmids (wild-type human PMS2 or PMS2 Kozak variants) were individually transfected into HEK293TK cells, grown for 48 hours, and translation efficiency was determined as the ratio of renilla/firefly expression using the Dual-Glo® Luciferase Assay (Promega).

Results/Data: Besides the 1A>C variant, which is already known to be pathogenic, we identified six additional variants that are likely pathogenic. In addition, we classified nine variants as likely benign. In the case of the c.-7T>C Kozak sequence variant, we identified no significant difference between this variant and the wild-type human PMS2 sequence supporting a benign clinical classification.

Conclusions: In summary, we present a novel method for the high-throughput classification of human PMS2 Kozak sequence variants that can contribute to the re-classification of VOUSs identified in human patients.

JUKEBOX: QUANTIFYING NOISE IN CHROMATIN COFORMATION CAPTURE MATRICES

Timothy Reznicek, Dr. Jordan Rowley
University of Nebraska Medical Center
Omaha, Nebraska

Background: Recent advances in 3D genome organization studies, facilitated by techniques such as Hi-C, Micro-C, and Pore-C, have enabled the measurement of long-range chromatin interactions. These interactions are commonly visualized as 2D heatmaps known as chromatin conformation capture matrices or contact maps, which are instrumental in understanding the spatial organization of chromatin within the nucleus. Distinct chromatin organization patterns have been observed across various cancer types, during cell differentiation, and in relation to gene expression. However, interpreting these matrices is often challenged by noise resulting from technical artifacts, sequencing depth variations, and experimental variability. We present a novel analytical tool designed to robustly estimate noise in contact maps, thereby enhancing their clarity and interpretability.

Significance: To date, no existing tool specifically quantifies noise in contact maps. Prior studies have acknowledged noise presence through visual inspection, which is subjective. Noise can obscure critical features in contact maps, such as chromatin loops and compartment boundaries, making quantification essential for accurate and reproducible data interpretation.

Hypothesis: We hypothesize that the inverse of the absolute value of the autocovariance function can effectively quantify noise in chromatin conformation capture matrices.

Experimental Design: Our approach, embodied in a tool named JUKEBOX, defines noise in contact matrices as bin-to-bin variance. It employs the inverse of the absolute value of the autocovariance function derived from matrix rows to model noise across the matrix. This method leverages the inherent spatial information within the chromatin conformation matrices for a statistically sound noise estimation. JUKEBOX's efficacy was tested under varying technical conditions, read depths, and experimental protocols to validate its robustness.

Results: JUKEBOX demonstrates high accuracy and reproducibility in estimating unique noise levels for each experiment's contact maps. Key findings include a decrease in noise with increased read depth, noise reduction upon data normalization in contact matrices, and protocol differences leading to varying noise levels. Notably, higher noise impairs the identification of chromatin loop features. We also introduce a novel subsampling method to correlate read depth with noise, refining noise estimation and providing vital insights into overall noise behavior.

Conclusion: This study introduces a comprehensive framework for noise estimation in chromatin conformation data, poised to substantially improve data reliability. JUKEBOX is expected to be a valuable resource for researchers exploring chromatin organization, furthering our understanding of genome architecture's impact on gene regulation and various disease states.

ESTABLISHING MOLECULAR REQUIREMENTS FOR ERYTHROID PROGENITOR ACTIVATION DURING ANEMIA RECOVERY

Pooja Roy[1], Suhita Ray[1], Suyong Choi[1], Kyle J. Hewitt[1].

[1]University of Nebraska Medical Center, Omaha, Nebraska.

Background: The sterile alpha motif-containing protein 14 (Samd14) protein boosts the erythroid system's potential for regeneration after anemia. Samd14 has a conserved sterile alpha motif (SAM) which is required for anemia-dependent SCF/Kit signaling, survival and colony-forming activity of erythroid precursor cells (EPCs). SAMs are among the most abundant modular domains found in eukaryotic proteins. Many SAMs are self-interacting and can form SAM-SAM oligomers and polymers. SAMs in a small fraction of proteins can bind DNA, RNA and lipids. However, there is no known interacting partner for Samd14-SAM. Samd14 does not dimerize, and mass spectrometric studies previously done in our lab revealed that its SAM domain does not interact with other SAMs. Sequence alignment of Samd14-SAM from different vertebrate species revealed an evolutionarily conserved polybasic motif (PBM) located within its SAM. PBMs are clusters of basic amino acids that many proteins utilize to engage in electrostatic interactions with the phosphate head group of phospholipids. We designed a Samd14 PBM-mutant (S14R381Q) to investigate the requirement of Samd14 interaction with phospholipids for promoting EPC activity during anemia recovery.

Significance of Problem: Identification of interacting partners for Samd14-SAM domain will resolve a major gap in knowledge regarding the molecular mechanisms by which homeostasis is restored by Samd14 after anemia. Mechanistic insights into cellular pathways controlling EPC survival and activation after anemia may potentially uncover novel clinical strategies for tackling dysregulated erythropoiesis.

Hypothesis: We hypothesize that SAM-dependent Samd14 interaction with phospholipids facilitates survival and signaling in erythroid progenitor cells during anemia recovery.

Experimental Design: To test if Samd14 interacts with phospholipids, we performed a protein-lipid overlay assay called PIP strip assay. HA-tagged full length Samd14, HA-tagged SAM-deleted mutant and HA-tagged S14R381Q was immunoaffinity purified from proerythroblast cells and overlaid on PIP strips. Protein-lipid interaction was detected by immunoblotting with Samd14 antibody. The sequence requirements for Samd14-PI3P interaction were validated in proerythroblast cells using proximity ligation assays (PLA). PI3P is enriched on endosome/autophagosome membranes, and it regulates multiple cellular processes like endocytic trafficking, protein sorting, receptor recycling and autophagy. To study the role of PI3P in erythropoiesis, we will inhibit Vps34 activity, the only known phosphatidylinositol-3 kinase required for PI3P synthesis. SAR405 is a potent and specific inhibitor of Vps34 activity. EPCs derived from mouse E14.5 fetal liver can differentiate to mature red blood cells in erythroid expansion media supplemented with SAR405 and with or without exogenous Samd14 expression. Effects of inhibiting Vps34 activity on erythroid maturation were determined using flow cytometry, morphological assessments and qRT-PCR.

Results: We found that full length Samd14 binds PI3P, as determined by PIP strip and proximity ligation assays. Compared to full length Samd14, the number of PLA puncta decreased by 3.3-fold in the absence of the SAM domain and by 1.9-fold in PBM mutant (S14R381Q). Thus, we have identified an arginine residue (R381) within Samd14-SAM which promotes PI3P interaction. Flow cytometry analysis with erythroid cell markers showed that Vps34 inhibition (using 5μM SAR405 treated cultures for 3 days) increased the numbers of undifferentiated erythroid precursors compared to controls. They express more cell surface Kit receptor and have significantly higher levels of *Gata2* transcripts, both of which are characteristic of more primitive cells. SAR405-treated cultures have fewer mature erythroid cells and significantly decreased levels of globin transcripts compared to controls. Taken together, our studies involving SAR405 indicated that inhibition of Vps34 activity leads to a block in terminal erythropoiesis.

Conclusions: Our data shows that Samd14 requires an arginine residue located within its SAM domain to bind PI3P. Preliminary studies show that inhibition of the Vps34 activity, the enzyme required for PI3P synthesis, blocks terminal erythropoiesis. Moving forward we will test whether the Samd14-PI3P interaction controls EPC survival, activity, Kit signaling and/or recycling in mouse anemia recovery models, using genetic complementation approaches with WT Samd14 or S14R381Q expression constructs. This work will broaden our understanding of cellular pathways controlling EPC survival and activation after anemia and establish the mechanism by which Samd14 alleviates anemia symptoms.